Solubility of H2 in water and NaCl brine under subsurface storage conditions: measurements and thermodynamic modeling

Salaheddine Chabab, Halla Kerkache, Ilias Bouchkira, Marie Poulain, Olivier Baudouin, Édouard Moine, Marion Ducousso, Hai Hoang, Guillaume Galliéro, Pierre Cézac

Solubility of H_2 in water and NaCl brine under subsurface storage conditions: measurements and thermodynamic modeling

Salaheddine Chabab [a,b,*], Halla Kerkache [a], Ilias Bouchkira [b,c], Marie Poulain [b], Olivier Baudouin [c], Édouard Moine [c], Marion Ducousso [b], Hai Hoang [d,e], Guillaume Galliero [a], Pierre Cézac [b]

[a] Universite de Pau et des Pays de l'Adour, E2S UPPA, CNRS, Total, LFCR, Anglet ou Pau ou Mont-de-Marsan, France

[b] Universite de Pau et des Pays de l'Adour, E2S UPPA, LaTEP, Pau, France

[c] ProSim SA, Immeuble Strategie A, 51 rue Ampere, F-31670 Labege, France

[d] Institute of Fundamental and Applied Sciences, Duy Tan University, Tran Nhat Duat Street, District 1, Ho Chi Minh City, Vietnam

[e] Faculty of Environmental and Natural Sciences, Duy Tan University, 03 Quang Trung Street, Da Nang, Vietnam

*Corresponding authors:

salaheddine.chabab@univ-pau.fr (S. Chabab)

Journal:

International Journal of Hydrogen Energy

Abstract

In the context of Underground Hydrogen Storage (UHS), deep saline aquifers offer great potential due to their availability and high storage capacity. In these porous media, the direct contact between gas (H_2), brine and rock can lead to biotic and/or abiotic reactions (e.g. Hydrogen-induced calcite dissolution, (bio)methanation, Acetogenesis, etc.). These reactions take place in the aqueous phase between dissolved species (gas and minerals), hence the need for accurate high-pressure solubility data of hydrogen in brine. At high-pressure conditions, only few data on the phase equilibria of H_2/brine systems are available in the open literature, and with significant inconsistencies among themselves. Hence, in this work, new solubility data for H_2 in NaCl brine were obtained under subsurface storage conditions using a volumetric method, at temperatures between 298 and 373 K, at NaCl molalities between 0 and 4mol/kgw, and at pressures up to 200 bar. Interestingly, the data measured in this work lies between the two existing data sources which exhibited noticeable discrepancies. These data were used to parameterize and evaluate three well-known thermodynamic models based on different approaches: e-NRTL activity coefficient model, Duan-type (non-iterative) model and Søreide and Whitson's equation of state. It has been found that these models, of which the advantages and limitations of each have been discussed, are able to provide highly accurate predictions of the phase equilibria of the H_2-NaCl brine system with an average absolute deviation of less than 3%. The resulting models and parameters can be used in reservoir simulators to evaluate dissolution losses and geobiochemical reactivity associated with UHS in porous media. Moreover, these models can be applied to estimate the saturation moisture content of gases coming out of UHS facilities, or in other applications (PEM electrolyzer, electrochemical H_2 compressors, etc.).

Keywords:

H_2 solubility in brine, Underground Hydrogen Storage, water content, Duan model, electrolyte-NRTL, Measurement, thermodynamic Modeling

1. Introduction

The massive development and deployment of renewable Hydrogen (H_2) can be considered as the main solution for reducing anthropogenic CO_2 emissions [1]. The use of renewable energies such as solar and wind power is becoming increasingly widespread, and is likely to be accelerated by recent environmental and geopolitical crises. However, these clean energy resources have certain limitations, such as intermittency, seasonal fluctuations and geographical constraints. This means that the supply is less controlled and predictable when using renewable resources, compared with conventional energy production (coal, hydrocarbons, nuclear), since natural conditions (solar radiation and wind speed) are subject to fluctuation [2, 3]. To balance these emerging energy production systems, surplus electricity (when production exceeds demand) can be used to electrochemically separate water molecules into H_2 and O_2. In other words, electricity is stored in chemical form by producing renewable H_2: it's the Power-to-Gas concept. Therefore, the successful implementation of this approach necessitates the availability of a reliable and massive hydrogen storage solution. For that purpose, hydrogen can be injected into underground reservoirs such as depleted natural gas reservoirs, salt caverns, or aquifers [4]. Underground Hydrogen Storage (UHS) allows for large-scale and long-duration storage capabilities [5]. Depending on demand, hydrogen stored underground can be extracted and utilized in various ways. It can be converted back into electricity through fuel cells [6], offering a clean power source. Alternatively, hydrogen can be used as a feedstock in industrial processes or as a clean fuel for transportation [7].

Among the potential options for UHS, saline aquifers show great promise as a viable solution for large-scale hydrogen storage. Aquifers are natural porous reservoirs saturated with saline water and sealed by an impermeable cap rock that prevents the gas from migrating to the surface [8]. They offer ample capacity, long-term storage capabilities (satisfying seasonal energy demands), and widespread geographic availability [4, 9, 10]. Following injection of H_2 into the aquifer, several physicochemical and biochemical processes can arise, influencing its stability and mobility, such as dissolution, diffusion, and reactivity [3, 5]. The dissolved hydrogen can react with dissolved minerals or even favor the dissolution of certain rock minerals. Even at low temperatures and under abiotic conditions, hydrogen can still be reactive, e.g. reducing pyrite to pyrrhotite and producing H_2S [11, 12], or dissolving calcite or siderite and producing CH_4 [13-16]. Under biotic conditions, it is even worse, since these and other reactions can be catalyzed by biological activity under current storage conditions (low temperature and high pressure) [17, 18]. Reactivity is one of the main concerns in UHS, as it leads to loss of H_2,

contamination of the gas with H_2S (highly corrosive and toxic gas) and CH_4 (change in purity), as well as alteration of the integrity of the caprock through dissolution of its minerals [18, 19]. Given the limited understanding of hydrogen's behavior in this storage media, it becomes essential to examine the diverse phenomena that may impact the integrity of the storage. To effectively study and develop such infrastructure, it is crucial to have a comprehensive understanding and quantification of the involved thermophysical properties, including gas/liquid solubility, diffusion, interfacial tension, and others. For instance, gas/brine mutual solubilities data are essential to calibrate the thermodynamic models used in compositional reservoir simulators to simulate fluid flow and transport in the reservoir [10, 20]. Moreover, the solubility of H_2 determines the potential of its reactivity since it occurs in the aqueous phase between dissolved species [18, 21], whereas without the presence of water it is very negligible [22]. On the other hand, fluid-fluid and solid-fluid interfacial tension (IFT) plays key role in storage capacity and confinement security [8, 23], as it enables the calculation of : i) maximum storage height [24]; ii) capillary pressure, which is the pressure that must not be exceeded to avoid capillary breakthrough and leakage of H_2 to the surface; iii) capillary number (ratio of viscous to interfacial tension effects) which is an important parameter in the performance of hydrogen flow in the reservoir [25].

Gas solubility in the aqueous phase is not only important for studying mobility and reactivity, but also for measuring and estimating other important thermophysical properties (i.e. density, IFT, viscosity, etc.) [10, 26]. Concerning the solubility of hydrogen in brine, due to the complexity, cost and hazardous nature, only two high-pressure experimental studies are available in the literature (Chabab et al. 2020 [27] and Torín-Ollarves and Trusler 2021 [28]), with major inconsistencies between them (up to 38%). Therefore, further experimental measurements are necessary to evaluate existing data and validate or refine thermodynamic models.

Hence, in this work, new experimental solubility data of hydrogen in brine (H_2O+NaCl) obtained with a different apparatus and protocol than the one used in our previous work (Chabab et al. 2020 [27]), are presented in section 2. Then, the measured data are used to adjust thermodynamic models using different approaches (gamma-phi and phi-phi) in section 3. In this last section, the different measurement methods used in the literature and in this work are compared and analyzed. Moreover, different thermodynamic models are fitted on the selected experimental data from the literature and this work, and the influence of the different parameters (temperature, pressure and salinity) on H_2 solubility, is studied.

2. Experimental

In order to determine the solubility of gases in water, various techniques have been developed and can be categorized as either analytical or synthetic methods [29]. Analytical (direct) methods such as volumetric, chromatography, and titration are commonly used to determine the composition of phases at thermodynamic equilibrium by analyzing samples outside the equilibrium cell. However, it is also possible to conduct compositional analysis inside the equilibrium cell itself without the need for taking samples (e.g. in-situ Raman-spectroscopy [30]). Synthetic approaches such as bubble point and material balance methods, do not necessitate any sampling, but they do require a very precise preparation of the mixture with known quantities before introducing it into an equilibrium cell.

Concerning the solubility of H_2 in brine at high pressure, only two experimental studies exist to date in the open literature (see Table 1). Chabab et al. 2020 [27] used the static analytical method (in-situ capillary sampling and gas chromatography analysis) to measure H_2 solubility in brine under storage conditions at different NaCl molalities (1-5 mol/kgw). Torín-Ollarves and Trusler 2021 [28] used a synthetic method based on bubble point pressure measurement in a constant-volume cell, to measure at a NaCl molality of 2.5 mol/kgw the H_2 solubility in brine. The authors reported a significant discrepancy between the two measurement sources.

Table 1 : High-pressure experimental solubility data for H_2 in brine: Comparison of operating ranges (pressure, temperature, salinity) of existing studies and this work

	Temperature (K)	Pressure (bar)	NaCl molality (mol/kgw)	Number of data points
Chabab et al. 2020	323 - 373	30 - 230	1 - 5	31
Torín-Ollarves and Trusler 2021	323 - 423	116 - 458	2.5	10
This work	298 - 373	100 - 200	1 - 4	37

The composition of a compound in a phase is a macroscopic thermodynamic property (bulk property), so generally, as sample size and number increase, so does the accuracy. This is because the measurement result becomes less impacted by dead volumes and inevitable micro-leaks during sampling, or is less impacted by the sensitivity limits of analytical equipment (chromatograph, gasometer, balance, titrator, etc.). Furthermore, the solubility of H_2 in brine is relatively small. Therefore, in this work, the volumetric/gravimetric method was chosen to

measure the solubility of H_2 in NaCl brine by analyzing relatively large samples (50-65 g) in order to limit as much as possible experimental error.

2.1. Materials

In Table 2, the suppliers of chemicals and the given purities are listed. Water was deionized and degassed before the gravimetric preparation of the brine (water + NaCl).

Table 2 : Chemicals description

Chemicals	Purity	Analytical Method	Supplier
H_2 (CAS Number: 1333-74-0)	99.999 vol%	GC: Gas Chromatography	Air Liquide
NaCl (CAS Number: 7647-14-5)	>99.5%	None	Thermo Scientific Acros

2.2. Apparatus and method

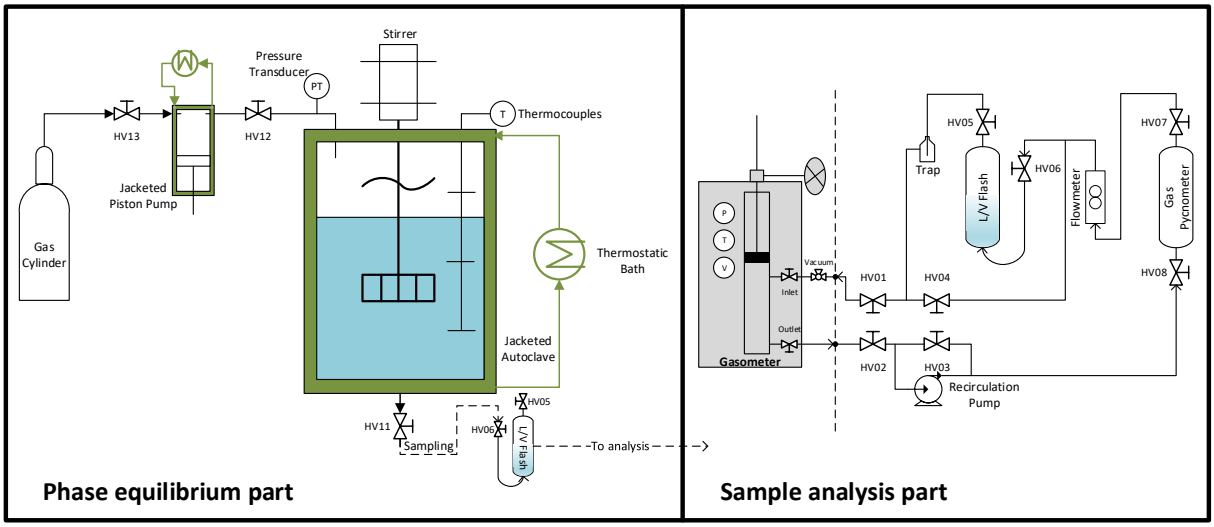

Figure 1: Scheme of the experimental setup used to measure H_2 solubility in brine

As shown in Figure 1, the experimental setup consists of a phase equilibrium part and an analytical part. The main idea to measure the H_2 solubility is to bring gas (H_2) and liquid (water or brine) into equilibrium in a stirred, instrumented autoclave (equilibrium cell). Once the pressure and temperature have stabilized, high-pressure samples of the gas-saturated liquid are taken from the bottom of the autoclave and degassed by expansion in a gasometer, enabling the gas that was dissolved under pressure to be quantified.

- Regarding the phase equilibrium part, it is the same equilibrium cell than the one used and presented in detail by dos Santos, et al. 2020 [31]. It is composed of an instrumented

equilibrium cell with pressure and temperature transducers and an agitator. A syringe pump from Irian Mecatronics (formerly ACEI Services) was used to inject a precise amount of gas into the cell. Before any use, the cell and the circuit of the equilibrium part are cleaned and put under vacuum.

The saline solution is injected by aspiration from the bottom of the cell, and the gas is injected from the top of the cell by the syringe pump until the desired pressure is attained. Equilibrium is considered to be reached after the stabilization of temperature and pressure (usually after 1 to 2 hours).

Once equilibrium is established, a sample (50-65 g) is taken from the bottom of the cell (liquid phase) using the L/V Flash for composition analysis. The size of the liquid sample is limited by the volume of the L/V Flash (75 cc). Therefore, in order not to fill the entire sample cylinder with gas-laden liquid, the sample volume is estimated using the amount of gas injected using the syringe pump to compensate and maintain a fixed pressure during sampling. During sampling, a pressure variation not exceeding ±0.1 bar was globally respected in order to avoid destabilizing the thermodynamic equilibrium (see Figure 2).

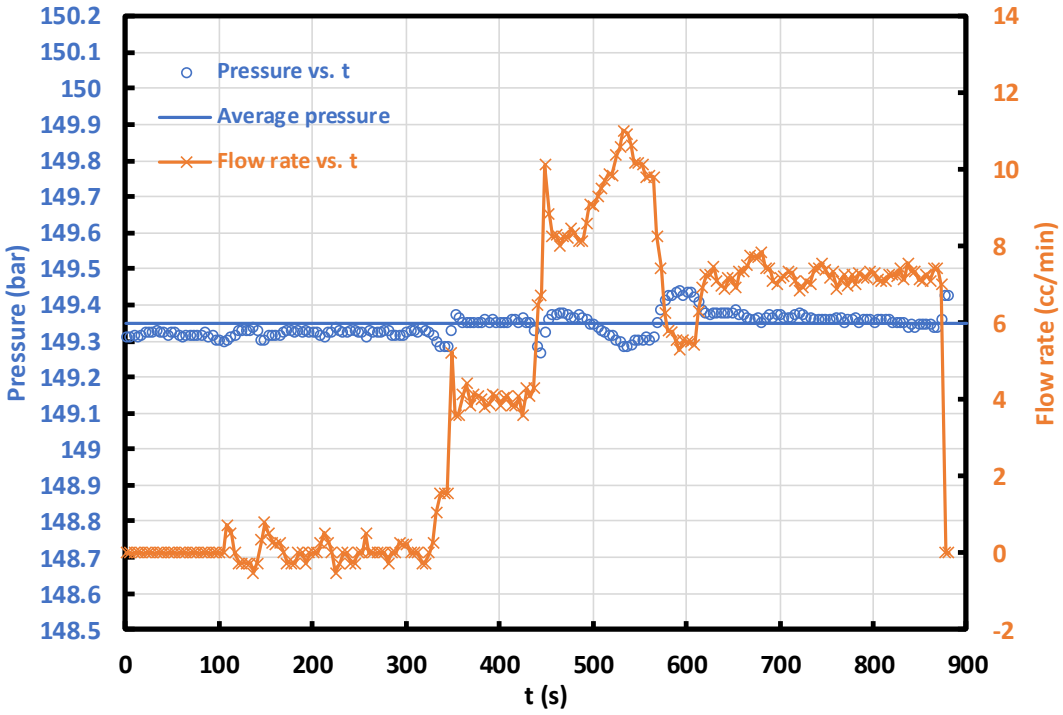

Figure 2: Pressure variation in the equilibrium cell during sampling

- For the analytical part, a volumetric/gravimetric method after flash separation under atmospheric conditions was used. The gas separated from the liquid by expansion in a

gasometer is quantified by the latter and the remaining liquid is measured by the difference in mass of the sample cylinder (L/V Flash) before and after sampling/degassing.

Furthermore, by measuring the mass of the sample cylinder before and after degassing, the quantity of the released gas can also be known gravimetrically, and thus compared with the results obtained volumetrically with the gasometer. However, this verification is only possible if one has a gas with a high solubility like CO_2 or H_2S, since one must have enough quantity of degassed gas for the gravimetric method to be reliable. Due to the low solubility of hydrogen (H_2) in brine, only the quantification (of the flashed gas) by gasometer has been considered in this work.

Prior to any data reading, equilibrium under atmospheric conditions is ensured by a recirculation pump that circulates the gas between the gasometer and the flash to achieve equilibrium.

$$x'_{H_2} = \frac{n_{H_2}}{n_{H_2} + n_{H_2O}} \quad \textbf{(1)}$$

The solubility of the gas (H_2) in the aqueous solution in terms of salt-free molar composition (x') in Equation (1) is obtained by calculating the mole numbers (n) of H_2 and H_2O at room conditions (hence the superscript R) using Equations (2) and (3).

$$\begin{aligned} n_{H_2} &= n^R_{H_2,aq} + n^R_{H_2,g} \\ n^R_{H_2,aq} &= \frac{x^R_{H_2,aq}}{1 - x^R_{H_2,aq}} n^R_{aq.sol.} \\ n^R_{aq.sol.} &= w_{H_2O} \frac{\left(M_f - M_i\right)}{Mw_{H_2O}} + \left(1 - w_{H_2O}\right) \frac{\left(M_f - M_i\right)}{Mw_{salt}} \\ n^R_{H_2,g} &= \left(1 - y^R_{H_2O,g}\right) \left(V_f - V_i - \frac{\left(M_f - M_i\right)}{\rho_{aq.sol.}} \right) \rho_{H_2} \end{aligned} \quad \textbf{(2)}$$

$$n_{H_2O} = n^R_{H_2O,aq} + n^R_{H_2O,g} = w_{H_2O} \frac{\left(M_f - M_i\right)}{Mw_{H_2O}} + y^R_{H_2O,g} \left(V_f - V_i - \frac{\left(M_f - M_i\right)}{\rho_{aq.sol.}} \right) \rho_{H_2} \quad \textbf{(3)}$$

In these equations, the subscripts "aq", "g" refer respectively to the aqueous phase and the gaseous phase where the component (H_2 or H_2O) is present. $n^R_{aq.sol.}$ represents the number of moles of the aqueous solution (water + salt) calculated from the mass difference $\left(M_f - M_i\right)$ of the sample cylinder between the initial state "i" (empty cylinder) and the final state "f" (cylinder containing the degassed aqueous solution) and the water mass fraction w_{H_2O}. The volume of the produced gas (by degassing the aqueous solution), is calculated from the volume difference

$(V_f - V_i)$ before and after degassing and by subtracting the volume occupied by the aqueous solution. In Equation (3), at room conditions "*R*" (temperature and pressure indicated by the gasometer), the mass density of the aqueous solution $\rho_{aq.sol.}$ (in [g/cc]) is calculated by the correlation of Al Ghafri et al. 2012 [32], and the molar density of H_2 (in [mol/cc]) by the hydrogen multiparameter reference model (Leachman et al. 2009 [33]) available on REFPROP (NIST software) [34]. The water content of the gas $y^R_{H_2O,g}$ as well as the solubility of the residual dissolved gas in the saline solution $x^R_{H_2,aq}$ under room conditions are determined using the Equation of State (EoS) of Søreide and Whitson 1992 [35] with the parameters recently optimized by Chabab et al. 2021 [36].

The salt-free molar composition (x') (Equation (1)) can be converted in terms of molality m_{H_2} (in [mol/kgw]) by the following relationship:

$$m_{H_2} = \frac{1000\, x'_{H_2}}{M_{H_2O}(1 - x'_{H_2})} \tag{4}$$

or in terms of "true" mole fraction by

$$x^{true}_{H_2} = \frac{n_{H_2}}{n_{H_2} + n_{H_2O} + n_s} = \frac{n_{H_2}}{n_{H_2} + n_{H_2O} + m_s n_{H_2O} Mw_{H_2O}} = \frac{x_{H_2}}{x_{H_2} + (1 - x_{H_2})(1 + m_s Mw_{H_2O})} \tag{5}$$

where n_s and m_s are respectively the salt mole number and molality (in [mol/kgw]), and Mw_{H_2O} is the water molecular weight (in [kg/mol]).

2.3. Experimental results

The solubility of H_2 in NaCl brine was measured at temperatures between 298 and 373 K, at NaCl molalities from 0 to 4 mol/kgw and pressures up to 200 bar. These measurement conditions are a compromise between typical subsurface storage conditions (porous media, in particular aquifers) and the maximum pressure limit of the autoclave used, which is 200 bar. That's one of the reasons why this part will be followed by a modeling part (section 3), which will complete the measurement gaps and extrapolate with more or less confidence beyond the measurement range, depending on the model chosen.

Measurement results are listed in Table 3, together with the associated expanded uncertainties $\mathbf{U}(\mathbf{x'_{H_2}}) = \boldsymbol{U_{expanded}}$ (k=2). The uncertainties were calculated using the method proposed by

NIST [37] and subsequently developed by Ahmadi and Chapoy 2018 [38] for the CO_2/brine system and who used the same measurement method (volumetric/gravimetric). Two sources of uncertainty are involved in the calculation of $\boldsymbol{U_{expanded}}$ (Equation 6):

- the first ($\boldsymbol{U_{measurements}}$) contains all the errors induced in the solubility calculation using equations 1-3 (including balance and gasometer errors, and errors resulting from the calculation of density and solubility at ambient pressure using equations of state, …).

- the second ($\boldsymbol{U_{repeatability}}$) is the uncertainty linked to the repeatability of measurements, which is checked regularly by measuring the same equilibrium point several times and calculating the mean standard deviation.

$$U_{expanded} = 2 \times \sqrt{U^2_{measurement} + U^2_{repeatability}} \quad \textbf{(6)}$$

The calculation of each term is detailed in the work of Ahmadi and Chapoy 2018 [38]. The only difference with their measurement method (and consequently the uncertainties) is the inclusion in this work of gas recirculation after atmospheric degassing. Unlike direct flash (without recirculation), gas recirculation ensures thermodynamic equilibrium and that no oversolubilized gas remains in the liquid (water or brine) [39]. After recirculation, only the amount of gas at the saturation state remains dissolved, which is easily quantifiable and taken into account in calculations, hence, repeatability is much improved. In this work, a repeatability uncertainty of less than 0.00002 was achieved. Finally, from the measured solubilities and the corresponding (absolute) extended uncertainties (Table 3), the relative uncertainties are ranging from 1% (in pure water) to 3.5% (in highly concentrated brine).

These measurement, compared with the only two data sources from the literature (Chabab et al. 2020 [27] and Torín-Ollarves and Trusler 2021 [28]), are analyzed in section 3.4.

Table 3: Measured solubility of H_2 in the H_2O + NaCl solutions, expressed as "salt-free" mole fractions (Eq. (1)).

m_{NaCl} (mol/kg_w)	T (K)	P (bar)	x'_{H_2}	$U(x'_{H_2})$
0	298.20	100.01	0.00135994	0.000023
0	298.05	150.01	0.00199679	0.000026
0	298.15	200.01	0.00264397	0.000030
0	298.15	200.01	0.00263320	0.000031

0	323.55	101.11	0.00125091	0.000023
0	323.50	101.31	0.00123925	0.000025
0	323.85	130.01	0.00159253	0.000026
0	323.55	165.01	0.00201117	0.000030
0	323.30	199.91	0.00244186	0.000036
0	323.35	200.11	0.00245479	0.000032
0	373.85	100.01	0.00142471	0.000024
0	373.80	100.01	0.00140332	0.000024
0	373.85	100.01	0.00140893	0.000024
0	373.65	175.11	0.00243347	0.000029
1	298.20	100.71	0.00107012	0.000022
1	298.30	150.01	0.00159298	0.000024
1	298.15	150.01	0.00161244	0.000024
1	298.30	200.01	0.00213575	0.000027
1	323.20	100.31	0.00102099	0.000022
1	323.40	100.61	0.00102078	0.000022
1	323.35	101.01	0.00102426	0.000022
1	323.20	150.06	0.00151377	0.000024
1	323.30	175.01	0.00176728	0.000024
1	323.30	199.91	0.00202590	0.000027
1	323.20	200.01	0.00204487	0.000028
1	373.25	100.11	0.00119671	0.000022
1	373.40	126.01	0.00148492	0.000023
1	373.10	150.36	0.00175595	0.000024
1	373.15	150.46	0.00179573	0.000026
1	373.45	150.71	0.00177350	0.000025
1	373.15	175.51	0.00204000	0.000026
1	373.00	200.46	0.00234604	0.000027
2	298.15	100.01	0.00088640	0.000021
2	298.05	150.01	0.00132235	0.000022
2	298.05	200.01	0.00171848	0.000024
2	323.20	100.01	0.00088260	0.000021
2	323.40	150.01	0.00131242	0.000022
2	323.35	150.01	0.00128912	0.000022
2	323.40	200.01	0.00172402	0.000024
2	373.05	100.01	0.00099379	0.000022
2	373.20	150.01	0.00151866	0.000023
2	373.40	200.51	0.00205031	0.000025
4	298.20	100.01	0.00059422	0.000021
4	298.20	150.01	0.00093595	0.000021

4	298.15	200.01	0.00121838	0.000022
4	323.30	100.01	0.00061736	0.000021
4	323.40	150.01	0.00095752	0.000021
4	323.40	200.01	0.00129237	0.000022
4	373.25	100.01	0.00077991	0.000021
4	373.35	150.01	0.00114509	0.000022
4	373.15	200.01	0.00157469	0.000023

3. Thermodynamic modeling

In this section, the vapor-liquid equilibria data of H_2+H_2O+NaCl from literature and those measured in this work are modeled using the asymmetric (gamma-phi) and symmetric (phi-phi) approaches, at different temperature, pressure and salinity conditions.

In the gamma-phi approach, the deviations from ideality in the liquid and vapor phases are represented by an activity coefficient using excess Gibbs energy (g^E) model and by a fugacity coefficient (using an EoS), respectively. The models following this approach that are used/developed in this work include:

- **model 1:** electrolyte Non-Random Two Liquid (e-NRTL), which has been chosen for its solid theoretical foundation and its ability to determine the chemical speciation (pH, concentration of species in solution, dissolution/precipitation, etc.) of a wide variety of electrolytic systems.
- **model 2:** Duan-type (Pitzer), which is widely used in the geochemistry community (e.g. phreeqc [40]) and represents a compromise between simplicity and reliability.

In the phi-phi approach, the deviation from ideality in the liquid and vapor phases is represented by a fugacity coefficient and generally by the same EoS. The parameters of the well-known Søreide-Whitson **(model 3)** have been reoptimized considering the new data. Unlike the two previous models, model 3 does not allow for the calculation of chemical speciation of non-molecular species (e.g. ionic species), but it does consider the effect of salinity on phase equilibrium (salting-out effect) between molecular species. This model was chosen because it is widely used in the oil and gas industry for hydrocarbon/gas/brine systems, and is implemented in most compositional reservoir simulators.

In contrast to model 2, which is non-iterative and provides directly the solubility of the gas in the liquid phase and its composition in the vapor phase, the compositions in the different phases (*x*: in liquid phase and *y*: in vapor phase) obtained by models 1 and 3 are obtained by means of phase equilibrium algorithms. In brief, the phase equilibrium in a vapor-liquid system is defined by the equality $f_{i,L} = f_{i,V}$ of the fugacities (*f*) of the components *i* between the vapor phase (*V*) and the liquid phase (*L*). This is equivalent to iteratively finding the compositions *x* and *y* that satisfy this constraint by specifying the temperature (*T*) and pressure (*P*) as input (*TP* flash calculation), or finding the corresponding *P* and *y* by specifying *x* and *T* (bubble point calculation), and so on. Thus, the role of thermodynamic models (1 or 3, for example) here is to calculate the fugacities of the compounds in the both phases at each iteration. These classical methods of resolving phase equilibria can be found in most thermodynamics' books [41-44].

3.1. Model 1: electrolyte–NRTL

The modeling of electrolyte solutions involving a dilute gas represents one of the new challenges in many fields of thermodynamics (gas treatment, hydrogen or ammonia production, …), due to the strongly non-ideal behavior of the mixtures (particles charged electrically, electrostatic interactions, presence of vapor-liquid, solid-liquid and chemical reaction equilibria). The electrolyte-NRTL (e-NRTL) model [45, 46] has proven recently to be a powerful tool, often selected for modeling the non-ideality of the liquid phase of this type of mixtures [47-57].

This activity coefficient model is based on the two-following hypothesis: 1. The repulsion between ions whose charges are of the same sign: the local composition (LC) of a cation (respectively an anion) near a cation (respectively an anion) is supposed to be zero. 2. Local electroneutrality: the anion and cation distribution around a central solvent molecule is as the local ionic strength is zero.

As a final result, the activity coefficient γ_i of each component *i* (solvent, anion or cation) is the sum of three different contributions (Equation 7): the NRTL term for local contribution, the Pitzer-Debye-Hückel (PDH) term [53] for long-range interaction contribution, and the Born term [54, 55] to make up for the difference between the reference state of the PDH term (infinite dilution in the mixed solvent) and the reference state of the local contribution term (infinite dilution in aqueous solution). This term is equal to 0 for solvents. Note that the latter term has no influence when considering systems containing only water as a solvent.

$$\ln(\gamma_i) = \ln\left(\gamma_i^{PDH}\right) + \ln\left(\gamma_i^{LC}\right) + \ln\left(\gamma_i^{Born}\right) \quad \textbf{(7)}$$

In this work, the τ and α parameters of water-gas and gas-ion pair involved in the local contribution term of the e-NRTL model were regressed by minimizing the Least Square Error between vapor-liquid equilibria experimental data and model's calculation. The Peng-Robinson EoS with the classical Van der Waals mixing rule [56] was selected to take into account the non-ideal behavior of the vapor phase.

This study was performed using *Simulis Thermodynamics* software [58, 59], the ProSim calculation server for thermophysical properties and phase equilibria calculations, in which the refined version of e-NRTL model developed by Song & Chen [57] is available. In this version, the Gibbs free energy formulation of the local contribution term has been developed on a generalized basis (ignoring the reference state), resulting in a simpler formulation that does not involve the "ionic charge fraction quantities".

3.2. Model 2: Duan-type (Pitzer)

Zhu et al. 2022 [60] proposed a heterogeneous non-iterative model following the Duan-type approach [61], using Pitzer's theory for aqueous electrolyte solutions for the liquid phase and Peng and Robinson's EoS [56] to calculate the fugacity coefficient φ_{H_2} of the gas (considered pure) in the vapor phase, as shown in Equation 8.

$$\ln\frac{y_{H_2}P}{m_{H_2}} = \frac{\mu_{H_2}^{l(0)}(T,P)}{RT} - \ln\varphi_{H_2}(T,P) + \sum_c 2\lambda_{H_2-c}m_c + \sum_c 2\lambda_{H_2-a}m_a + \sum_c\sum_a \zeta_{H_2-c-a}m_c m_a \quad \textbf{(8)}$$

where P and y_{H_2} are the total pressure (in bar) and mole fraction of H_2 in the gas-phase, respectively. m_{H_2} and $\mu_{H_2}^{l(0)}$ represent the molality (in mol/kgw) and chemical potential of H_2 in the liquid phase, respectively. R is the universal gas constant (83.14 bar.cm^3/mol/K) and T is the system temperature (in K). λ and ζ represent the second-order and third-order interaction parameters of the Pitzer's model [62], respectively.

The hydrogen composition (or water content) in the gas phase are estimated using a semiempirical expression (equation 9). The mole fraction of water in the liquid phase, denoted as x_{H_2O}, can be approximated as 1 in the H_2 + H_2O system and as $1–2x_{NaCl}$ in the H_2 + H_2O +

NaCl system, disregarding dissolved hydrogen. The saturation pressure $P_{H_2O}^{sat}$ and volume ${v'}_{H_2O}$ of water were calculated using the model developed by Wagner and Pruß 2002 [63]. The water fugacity coefficient φ_{H_2O} (equation 10) in the vapor phase is adjusted to reproduce the water content in the gas-rich vapor phase.

$$y_{H_2O} = 1 - y_{H_2} = \frac{x_{H_2O} P_{H_2O}^{sat}}{\varphi_{H_2O} P} \times \exp\left(\frac{{v'}_{H_2O}\left(P - P_{H_2O}^{sat}\right)}{RT}\right) \quad \textbf{(9)}$$

$$\varphi_{H_2O} = \exp(A_1 + A_2 P + A_3 P^2 + A_4 PT + \frac{A_5 P}{T} + \frac{A_6 P^2}{T}) \quad \textbf{(10)}$$

where A_1 – A_6 are empirical parameters to be adjusted on gas phase water content data.

Similar to Zhu et al. 2022 [60], by using the equation 11 proposed by Pitzer, the T-P dependencies of λ, ζ, and $\frac{\mu_{H_2}^{l(0)}(T,P)}{RT}$ are taken into account.

$$\mathrm{Par}\,(T,P) = C_1 + C_2 T + \frac{C_3}{T} + C_4 T^2 + C_5 P + \frac{C_6 P}{T^2} + \frac{C_7}{P} + C_8 \frac{T}{P} + C_9 \frac{T^2}{P} + C_{10} \frac{T^3}{P} \quad \textbf{(11)}$$

where C_1 – C_{10} are empirical parameters to be adjusted on gas solubility in aqueous phase data.

In this study, new experimental data were obtained for the solubility of H_2 in NaCl solution, which deviate from the data used by Zhu et al. 2022 for optimization of the model parameters. Therefore, the parameters λ_{H_2-c} and ζ_{H_2-c-a} of this semi-empirical model were readjusted based on the new and some literature data (Braun 1900 [64] and Crozier & Yamamoto 1974 [65]).

Furthermore, in the equation 10, Zhu et al. 2022 kept the coefficients taken from the vapor phase data (dew curve) of the CH_4-H_2O system and not H_2-H_2O. Therefore, in a similar way, the parameters A_1 – A_6 for calculating the water content in the vapor phase (Equations 9-10) were readjusted in this work to the dew-curve data for the H_2-H_2O system from Gillespie and Wilson 1980 [66]. The revised model parameters for H_2 solubility and water content in the H_2-rich phase are listed in Table 4.

Table 4 : Optimized coefficients for H_2 solubility in brine and water content in gas phase calculation using model 2 (Duan-type)

Equation 11					Equation 10	
Parameters	$\frac{\mu_{H_2}^{l(0)}}{RT}$	λ_{H_2-c}	λ_{H_2-a}	ζ_{H_2-c-a}	Parameters	Values
C1	41.8266086	-7.74829265312071	0	-0.009470244669	A1	-0.0183687889210319
C2	-8.24713967*(10^-2)	0.0226221702021589			A2	0.0258865530837438
C3	-4.60318630*(10^3)	923.092396500207			A3	-1.97530641525822e-05
C4	6.03537635*(10^-5)	-2.21140172559128e-5			A4	-3.10454712930491e-05
C5	4.12979459*(10^-4)	7.40868321886585e-5			A5	-5.61575502087305
C6	1.82081207*(10^1)	-12.3509724808910			A6	0.00673250140185062
C7	3.73478602*(10^1)	-47.3816790140829				
C8	-3.87633253*(10^-1)	0.469165009435218				
C9	1.34370747*(10^-3)	-0.0015626314758				
C10	-1.55621990*(10^-6)	1.75015662317748e-6				

3.3. Model 3: Søreide and Whitson EoS

The Søreide and Whitson EoS [35] is widely utilized in the oil and gas industry, particularly for systems involving gas, water, and salt. It can be found in various thermophysical calculators, such as ProSim's *Simulis Thermodynamics* [58, 59], as well as most reservoir simulation codes (MUFITS [67], Eclipse 300 [68], IHRRS [69], etc.). Although the Søreide and Whitson EoS does not function as an electrolyte model, it considers the effect of salt on phase equilibria, specifically on the saturation vapor pressure of water and the gas/water mutual solubilities.

However, due to the use of two binary interaction parameters (k_{ij}^{AQ} for the aqueous liquid phase and k_{ij}^{NA} for the non-aqueous phase), the model is equivalent to an asymmetric approach and is therefore not suitable for mixtures near their critical point, such as in the presence of large amounts of CO_2 or H_2S under conditions close (or higher) to (than) the critical point of water. However, since the underground storage conditions are far from the critical point of water, this type of model can still be employed.

$$\left(k_{H_2-H_2O}\right)_{SW} = D_0(1+\alpha_0 m_{NaCl}) + D_1\frac{T}{T_{c,H_2}}(1+\alpha_1 m_{NaCl}) + D_2\exp\left(D_3\frac{T}{T_{c,H_2}}\right) \quad \textbf{(12)}$$

The coefficients D_x and α_x of equation 12 obtained by Chabab et al. 2020 [27] have been reoptimized on the new data and are listed in Table 5 with the corresponding average absolute deviations (on H_2 solubility x_{H_2} and water content in gas phase y_{H_2O}).

Table 5: Optimized coefficients of the binary interaction parameters in aqueous $k_{H_2-H_2O}^{AQ}$ and non-aqueous $k_{H_2-H_2O}^{NA}$ phases (Equation 12).

		$k_{H_2-H_2O}^{AQ}$	$k_{H_2-H_2O}^{NA}$
D_0		-2.11917	0.01993
D_1		0.14888	0.042834
D_2		-13.01835	-
D_3		-0.43946	-
α_0		-2.26322×10^{-2}	-
α_1		-4.4736×10^{-3}	-
T_{c,H_2}(K)		33.145	
AAD (%)	x_{H_2}	3.13	
	y_{H_2O}	2.49	

3.4. Modeling results and discussions

The three models cited above were used to process the data measured in this work and those from the literature. The results are presented in two sections. The first deals with the solubility of H_2 in water and brine, and the comparison of the salting-out effect of different gas. The second section is dedicated to the vapor phase, in particular the prediction of water content in H_2 in the presence or absence of salts.

3.4.1. Liquid phase: H_2 solubility in water and NaCl brine

Figures 3-A, 3-B and 3-C illustrate the results of the three model calculations plotted against the experimental solubility data. All three models reproduce similarly well the solubility of H_2 in pure water and NaCl brine, as compared to the experimental data obtained in this study. The salting-out effect due to the presence of NaCl and the effect of temperature and pressure are well captured by the models.

Model 2 (Duan-type) performs slightly better than the other models, but this is quite normal given that it is an empirical model with a pressure dependency in the activity coefficient model parameters, which is not the case with model 1 (e-NRTL), which only considers a temperature dependency in the model parameters. Unlike model 2, model 1 is a consistent model that can be used to estimate not only the solubility of pure gases, but also gas mixtures, salt mixtures, and chemical speciation (activity coefficient of dissolved chemical species, pH, etc.).

Depending on the application, one of these three models could be more appropriate. The first one is more sophisticated and is easily adapted to calculations of complex systems (mixtures of gases and electrolytes), but is complicated to implement. For this reason, *Simulis Thermodynamics* software was used in this work, as it offers considerable flexibility in model parameterization, with many parameters already available in the database for water/electrolytes and gas/water/electrolytes systems. The second model (Duan-type) has the advantage of being non-iterative and very simple to implement with considerable accuracy, but not easy to generalize and not suitable for mixtures of salts and gases without making it iterative (i.e. flash calculation). Model 3 (Søreide-Whitson EoS), is widely used in reservoir simulators where it would be too expensive to use a sophisticated and CPU time consuming calculation (like model 1). So, generally, in these cases reservoir water salinity is converted to NaCl equivalent for convenient use with model 3 which is already adapted to hydrocarbon/gas/water/NaCl mixtures [35, 36, 70].

To facilitate the choice of model according to the application and the type of information required, the advantages and limitations of these three models are summarized in Table 6.

Concerning the measurements carried out in this work, as observed in Figures 3A-C, the solubility measurements in pure water are in excellent agreement with those from the literature. However, this is not the case for the measurements of H_2 solubility in brine. To compare the measurements of this work with those of Chabab et al. 2020 [27] and Torín-Ollarves and Trusler 2021 [28], H_2 solubility is plotted as a function of NaCl molality at 323 K and 150 bar in the Figure 3-D. The results clearly show the dispersion of results (up to 38%) between the different data sources. In contrast to the results of Chabab et al. 2020, a much lower salting-out effect (decrease in H_2 solubility) is reported by Torín-Ollarves and Trusler 2021. The data measured in this work lies between the two literature data sources. With only 3 data sources, it is very difficult to identify consistent measurements from those with significant uncertainty. However, it is important to point out a few elements that should be considered by future studies on the subject of gas solubility in liquids in general, and also to possibly understand the cause of these discrepancies. The measurement methods used in the three studies should be recalled:

- Chabab et al. 2020 performed equilibrium in a cell and took micro-samples to be analyzed by gas chromatography. Two syringes of different volumes were used to calibrate the full range of measurements, and a non-linearity and non-continuity were observed in both calibration curves. The advantage of this technique is that sampling very small volumes does not affect thermodynamic equilibrium, and is carried out automatically in situ. However, results are highly dependent on chromatographic calibration, and a small error can induce considerable error in the measured composition.
- In the study by Torín-Ollarves and Trusler 2021, H_2 solubility was measured using a method for determining bubble point pressure in a fixed-volume equilibrium cell. This is achieved by introducing a known quantity of gas and proportionally injecting the aqueous phase until a bubble point is reached. The advantage of this synthetic method is that it is simple and does not require sampling, and the phase transition (bubble point) can be identified either graphically or by a physical model such as the one presented in their study, enabling cross-checking. However, it is necessary to control the quantities injected, which is usually done by syringe pumps connected to the equilibrium cell, which runs the risk of having a temperature gradient in the circuit (pump ==> transfer line ==> cell) that can impact on the accuracy of the quantities injected. Another challenge is that, since water is incompressible, a slight variation in its volume changes the pressure drastically.

- In this work, in contrast to the two previous methods, very large liquid samples are taken and analyzed "macroscopically" by volumetric (degassed H_2) and gravimetric (degassed brine) methods, after degassing the sample at atmospheric equilibrium. With this technique, given the sample size, a lower uncertainty is expected. However, care must be taken to ensure that atmospheric equilibrium is reached, as the amount of gas remaining dissolved and the moisture content of the degassed gas is estimated by a thermodynamic model at equilibrium. In this work, a gas recirculation is performed to reach equilibrium under atmospheric conditions to reduce the error. Another challenge is that, as very large samples are taken, care must be taken not to destabilize the system, by maintaining the fixed pressure in the equilibrium cell through automated (preferably) injection of gas from the top of the cell at the time of liquid phase sampling.

On the basis of these investigations, it can be inferred that the error induced by the destabilization of equilibrium due to small pressure fluctuations during sampling is less significant than the risk of strong dependence of results on calibration or the other difficulties just mentioned. For this reason, the data measured in this work have been selected to parameterize the proposed thermodynamic models.

The salting-out (SO) effect on gas solubility can be expressed in terms of Setschenow's constant [71], or by calculating the percentage decrease in solubility $SO = 100\left(\frac{x_{GAS}^{WATER} - x_{GAS}^{BRINE}}{x_{GAS}^{WATER}}\right)$ under the same thermodynamic conditions of T, P and salinity (Koschel et al. 2006 [72]). The calculations of the salting-out coefficients of H_2 according to the 3 existing studies and also of other gases of more or less similar sizes and solubility, are listed in Table 7. As the results show, CH_4, O_2 and N_2 have a very similar salting-out effect at both low (1m NaCl) and high (4m NaCl) salinities. In addition, interestingly, all three studies show less salting-out for H_2, especially the study by Torín-Ollarves and Trusler 2021 and this work. These characteristics are consistent with previous studies based on Setschenow's constant [73], even though these were carried out under low-pressure conditions (but the salting-out effect is barely affected by pressure). The difference in the salting-out effect is most likely an effect of molecular size, as exhibited by Noble Gases (see Ballentine et al. 2002 [71]], but possibly not only, since solubility is a multifactorial function [74]. Therefore, it will be interesting to carry out molecular simulations to try to understand the different behavior of aqueous hydrogen compared with other gases.

Finally, Table 8 tabulates the values of H_2 solubility in NaCl brine calculated by semi-empirical model 2 (Duan type) within the parameter fitting range (UHS conditions).

3.4.2. Vapor phase: water content in H_2-rich phase in the presence or absence of salts

Quantifying the water content in the gas phase is also an important property, especially for seasonal storage in porous media where the extracted gas will be quasi-saturated or saturated with water. Moreover, it is also an important data for other applications and processes [75, 76] (PEM electrolyzer, electrochemical hydrogen compressor, water-scrubbing, etc.). In Figure 4-A, the water content calculated by Model 1 and that calculated with the simple pseudo-empirical correlation (Equations 9-10) are compared with data from the literature (Gillespie and Wilson 1980 [66]). Model 1 and the pseudo-empirical correlation accurately estimate the water content in the vapor phase and can be used to predict the water content for the applications listed earlier.

For process simulation, where gas mixtures and possibly salt mixtures exist (for various applications, e.g. underground gas storage, geothermal energy, etc.), Model 1 (e-NRTL) is the one that can be used due to its strong theoretical basis. This model was also used to predict the effect of salt on water content in H_2 and the results are shown in Figure 4-B. The results show that salt (NaCl) also leads to a reduction in water content in the vapor phase, but to a lesser extent than the effect on H_2 solubility in the aqueous phase. It would be interesting in future studies to measure the effect of salt on water content to evaluate these predictions, but it is certain that salt (even at saturation, e.g. salt cavern) is far from being sufficient to reduce H_2 moisture to an acceptable level (5 ppm according to the ISO 14687−2:2012 standard), hence a dehydration step is certainly needed at the outlet of the storage well.

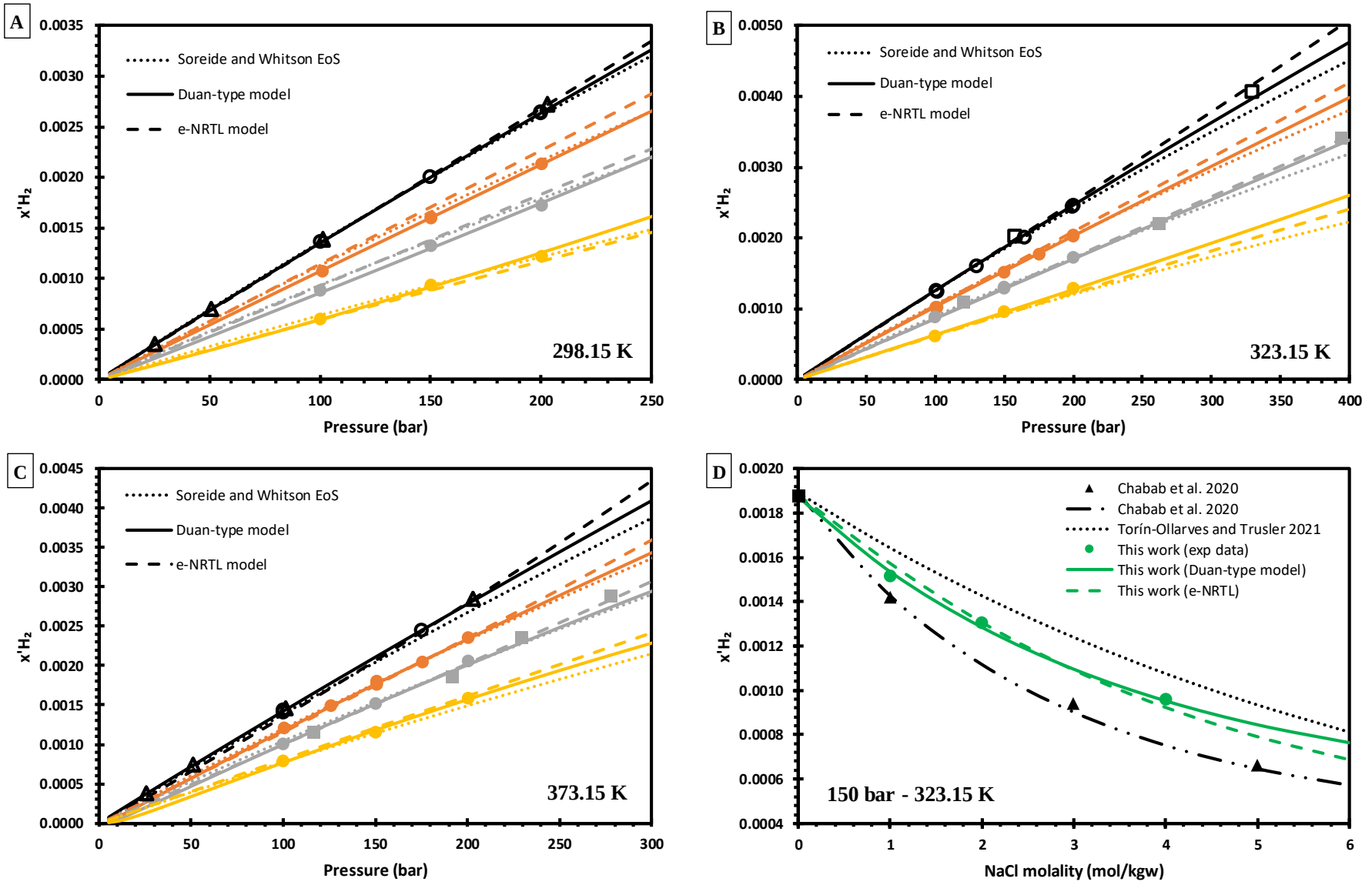

Figure 3: Solubility of H_2 in H_2O + NaCl at 298.15 K (A), 323.15 K (B) and 373.15 K (C) and different NaCl molalities (salt-free: black open-symbols and lines; 1m: orange filled-symbols and lines; 2m: grey filled-symbols and lines; 4m: yellow filled-symbols and lines). (D): Effect of NaCl on H_2 solubility according to different data sources. Literature data [27, 28, 77] are represented by squares and triangles and measured ones (Table 3) are represented by open and filled circles.

Table 6: Advantages and limitations of the models used in this work with regard to the calculation of phase equilibria of systems (hydrocarbons+gases+brine) relevant to UHS. Meaning of the different ratings: H: High; M: Medium; L: Low

	Applicability	Accuracy	Computational complexity	Remarks
model 1 (e-NRTL)	H	H	H	The model is (and can be) used in a wide variety of applications (multicomponent and multiphase systems). However, it is complicated to implement, but available in thermodynamic calculators and process simulators (e.g. *ProSimPlus*, *Simulis Thermodynamics*, *Aspen Plus*). Suitable for predicting properties beyond the parameter fitting range.
model 2 (Pitzer)	L	H	L	In its current form (as presented in this work): i) the model is very useful (non-iterative and simple to implement) for correlating data with a very high degree of accuracy, but only in the parameter fitting domain (extrapolation is risky with this type of empirical model); ii) it is not adapted to gas mixtures (requires the use of a flash calculation, for example, and therefore becomes iterative just like the other models).
model 3 (SW EoS)	M	H	M	The model can be extrapolated with less risk under UHS conditions. The model is not adapted for chemical speciation, but considers the effect of salinity (salting-out) on molecular species. Very suitable for mixtures of molecular compounds (hydrocarbons, gases, water), since it has only one adjustable parameter per binary compound and per phase, which makes it the simplest of the 3 models to parameterize, hence its widespread use in reservoir simulators.

Table 7: Salting-Out (SO) effect of different gas in NaCl brine

	NaCl molality (mol/kgw)	CH_4 [a]	O_2 [b]	N_2 [a]	H_2 [b]	H_2 [c]	H_2 (This work)
SO (%) at 323.15 K	1	25.35	25.38	25.24	24.28	13.10	16.23
	4	65.23	64.03	65.01	60.09	42.98	50.70

[a] calculated from O'Sullivan & Smith 1970 data [78]; [b] calculated from Chabab's 2020 smoothed data using e-PR-CPA model [27]; [c] calculated from Torín-Ollarves and Trusler 2021 [28] smoothed data using Krichevsky-Kasarnovsky model; $SO = 100\left(\frac{x_{GAS}^{WATER} - x_{GAS}^{BRINE}}{x_{GAS}^{WATER}}\right)$

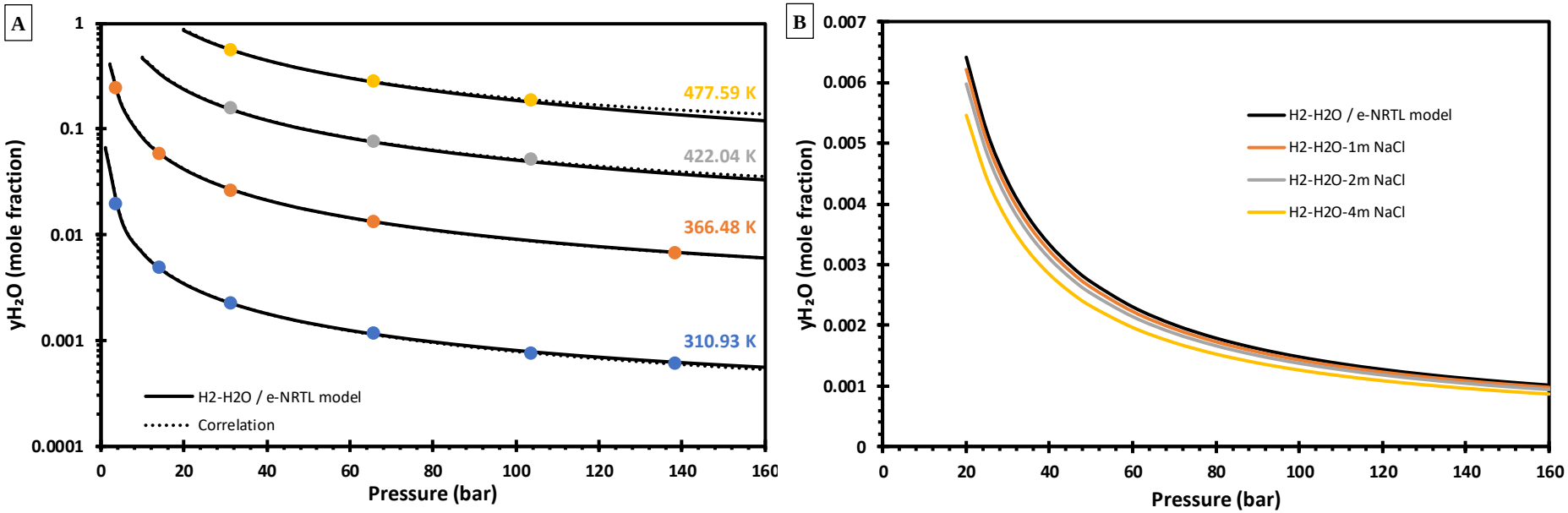

Figure 4: Vapor phase calculation: (A): water content in H_2-rich phase at 311, 366, 422, and 478 K. Comparison of literature data [66] represented by symbols, with predictions using the e-NRTL model and the semi-empirical correlation (Equations 9-10). (B): effect of NaCl on water content predicted using the e-NRTL model.

Table 8 : Calculated hydrogen solubility x'_{H_2} (salt-free mole fraction) in water + NaCl using the model 2 (Duan-type).

T (K)	P (bar)									
	5	10	15	20	25	50	75	100	150	200
m = 0 mol/kgw										
298.15	6.9429E-05	1.3874E-04	2.0782E-04	2.7667E-04	3.4529E-04	6.8518E-04	1.0201E-03	1.3506E-03	1.9997E-03	2.6356E-03
323.15	6.4671E-05	1.2933E-04	1.9379E-04	2.5806E-04	3.2214E-04	6.3982E-04	9.5329E-04	1.2629E-03	1.8720E-03	2.4692E-03
348.15	6.6532E-05	1.3301E-04	1.9923E-04	2.6524E-04	3.3108E-04	6.5763E-04	9.8014E-04	1.2989E-03	1.9264E-03	2.5419E-03
373.15	7.1062E-05	1.4446E-04	2.1700E-04	2.8920E-04	3.6115E-04	7.1799E-04	1.0705E-03	1.4189E-03	2.1050E-03	2.7779E-03
m = 1 mol/kgw										
298.15	5.3116E-05	1.0711E-04	1.6102E-04	2.1486E-04	2.6863E-04	5.3649E-04	8.0299E-04	1.0685E-03	1.5977E-03	2.1262E-03
323.15	5.4785E-05	1.0720E-04	1.5951E-04	2.1170E-04	2.6378E-04	5.2256E-04	7.7887E-04	1.0330E-03	1.5356E-03	2.0323E-03
348.15	4.5908E-05	1.0123E-04	1.5665E-04	2.1198E-04	2.6718E-04	5.4096E-04	8.1115E-04	1.0780E-03	1.6024E-03	2.1158E-03
373.15	2.6950E-05	8.3183E-05	1.4358E-04	2.0508E-04	2.6693E-04	5.7565E-04	8.8046E-04	1.1807E-03	1.7678E-03	2.3382E-03
m = 2 mol/kgw										
298.15	4.1434E-05	8.4312E-05	1.2722E-04	1.7014E-04	2.1310E-04	4.2830E-04	6.4447E-04	8.6188E-04	1.3014E-03	1.7487E-03
323.15	4.7321E-05	9.0603E-05	1.3387E-04	1.7708E-04	2.2024E-04	4.3517E-04	6.4884E-04	8.6147E-04	1.2844E-03	1.7053E-03
348.15	3.2297E-05	7.8552E-05	1.2559E-04	1.7274E-04	2.1984E-04	4.5372E-04	6.8446E-04	9.1213E-04	1.3589E-03	1.7955E-03
373.15	1.0420E-05	4.8834E-05	9.6866E-05	1.4828E-04	2.0116E-04	4.7058E-04	7.3838E-04	1.0017E-03	1.5137E-03	2.0066E-03
m = 4 mol/kgw										
298.15	2.6728E-05	5.5382E-05	8.4176E-05	1.1310E-04	1.4215E-04	2.8937E-04	4.4004E-04	5.9442E-04	9.1524E-04	1.2537E-03
323.15	3.7427E-05	6.8608E-05	9.9959E-05	1.3135E-04	1.6276E-04	3.1992E-04	4.7732E-04	6.3510E-04	9.5235E-04	1.2727E-03
348.15	1.6944E-05	5.0141E-05	8.5573E-05	1.2159E-04	1.5778E-04	3.3835E-04	5.1661E-04	6.9226E-04	1.0360E-03	1.3705E-03
373.15	1.6503E-06	1.7838E-05	4.6728E-05	8.2168E-05	1.2109E-04	3.3335E-04	5.5046E-04	7.6426E-04	1.1763E-03	1.5662E-03

Conclusions

Precise quantification of the solubility of hydrogen in brine at high pressure is of great importance, particularly for UHS or the exploration of natural hydrogen and the understanding of its underground generation. However, the very limited available data exhibit considerable inconsistencies, hence the relevance of this work. The aim is to carry out additional measurements using another experimental method and to provide reliable data for the calibration of existing models, thus enabling future research to better assess the phenomena that are impacted by H_2 dissolution during UHS.

New measurements of hydrogen solubility were carried out under conditions of high pressure (up to 200 bar), temperatures ranging from 298 to 373 K and salinities up to 4 mol/kgw of NaCl. The H_2 solubility in water and brine increase with pressure and follows Henry's law in a quasi-linear trend. Models optimized on experimental data predict a minimum solubility temperature ($T_{x_{H_2,min}}$) of around 326 K in pure water, decreasing with salinity ($T_{x_{H_2,min}} = 315$ K at 2m NaCl and $T_{x_{H_2,min}} = 288$ K at 4m NaCl). When compared with the solubility of other gases (N_2, O_2, CH_4) in brine under the same conditions, our data indicates a lower salting-out effect (decrease in solubility with increasing salinity) on hydrogen than on the other gases. This is most probably due to the small molecular size of hydrogen, which is less impacted by the solvation of ions by water molecules.

It is presumed that the new data have fewer uncertainties than existing data, given: i) the large sample size considered: The larger the sample, the less the measurement is affected by the measurement limits of the balance and gasometer; and ii) the sophisticated analysis technique used (recirculation flash), which considerably reduces uncertainty by improving repeatability. For this reason, these data have been considered to re-optimize the existing models (e-NRTL activity model and Søreide and Whitson EoS) available in *Simulis Thermodynamics* software and also to provide an easily implementable semi-empirical correlation model for fast and simple calculations.

The data obtained in this work, and more precisely the resulting models and parameters, can be used in reservoir simulators to improve the representation of species distribution between the liquid and gas phases, and to assess dissolution losses and geobiochemical reactivity associated with UHS in porous media. In addition, the tested thermodynamic models and the semi-empirical correlation accurately predict the water content in H_2-rich phase. Hence, they can be

used to estimate the moisture content of gases coming out of UHS facilities, or the humidity at the outlet PEM electrolyzer and electrochemical hydrogen compressors.

In UHS in porous media, H_2 is very likely to be present with other gases (cushion or reactively-produced gases such as H_2S or CH_4). In this case, it would be interesting to study the effect of gas mixing, and see whether this is simply an additive (ideal) behavior that is easily predictable by models 1 or 3, or whether a co-solubility effect exists due to the possible dissimilarity between these gases. Furthermore, it would be interesting to study other physical parameters that may affect the solubility of H_2 in porous media, such as the nature of the salt or even the presence of clay.

Acknowledgments

Financial support from the "HYDR" project partners is gratefully acknowledged. The S.C. "HYDR" Chair is funded by the ISITE E2S program, supported by ProSim SA, ANR PIA, IFPEN and Région Nouvelle-Aquitaine. The Institut Carnot "ISIFoR" is also gratefully acknowledged for financing the H2Stock Project.

References

[1] Agency IE. Global Hydrogen Review 2022: OECD Publishing; 2022.

[2] Kojima H, Nagasawa K, Todoroki N, Ito Y, Matsui T, Nakajima R. Influence of renewable energy power fluctuations on water electrolysis for green hydrogen production. Int J Hydrogen Energy. 2023;48:4572-93.

[3] Heinemann N, Alcalde J, Miocic JM, Hangx SJ, Kallmeyer J, Ostertag-Henning C, et al. Enabling large-scale hydrogen storage in porous media–the scientific challenges. Energy & Environmental Science. 2021;14:853-64.

[4] Raad SMJ, Leonenko Y, Hassanzadeh H. Hydrogen storage in saline aquifers: Opportunities and challenges. Renewable and Sustainable Energy Reviews. 2022;168:112846.

[5] Pan B, Yin X, Ju Y, Iglauer S. Underground hydrogen storage: Influencing parameters and future outlook. Adv Colloid Interface Sci. 2021;294:102473.

[6] Aminudin M, Kamarudin S, Lim B, Majilan E, Masdar M, Shaari N. An overview: Current progress on hydrogen fuel cell vehicles. Int J Hydrogen Energy. 2023;48:4371-88.

[7] Zuben TWV, Moreira DE, Germscheidt RL, Yoshimura RG, Dorretto DS, Araujo A, et al. Is hydrogen indispensable for a sustainable world? A review of H 2 applications and perspectives for the next years. Journal of the Brazilian Chemical Society. 2022;33:824-43.

[8] Hosseini M, Ali M, Fahimpour J, Keshavarz A, Iglauer S. Assessment of rock-hydrogen and rock-water interfacial tension in shale, evaporite and basaltic rocks. Journal of Natural Gas Science and Engineering. 2022;106:104743.

[9] Muhammed NS, Haq B, Al Shehri D, Al-Ahmed A, Rahman MM, Zaman E. A review on underground hydrogen storage: Insight into geological sites, influencing factors and future outlook. Energy Reports. 2022;8:461-99.

[10] Raad SMJ, Ranjbar E, Hassanzadeh H, Leonenko Y. Hydrogen-brine mixture PVT data for reservoir simulation of hydrogen storage in deep saline aquifers. Int J Hydrogen Energy. 2023;48:696-708.

[11] Truche L, Berger G, Destrigneville C, Guillaume D, Giffaut E. Kinetics of pyrite to pyrrhotite reduction by hydrogen in calcite buffered solutions between 90 and 180 C: Implications for nuclear waste disposal. Geochim Cosmochim Acta. 2010;74:2894-914.

[12] Truche L, Jodin-Caumon M-C, Lerouge C, Berger G, Mosser-Ruck R, Giffaut E, et al. Sulphide mineral reactions in clay-rich rock induced by high hydrogen pressure. Application to disturbed or natural settings up to 250 C and 30 bar. Chem Geol. 2013;351:217-28.

[13] Henkel S, Pudlo D, Werner L, Enzmann F, Reitenbach V, Albrecht D, et al. Mineral reactions in the geological underground induced by H2 and CO2 injections. Energy Procedia. 2014;63:8026-35.

[14] Bo Z, Zeng L, Chen Y, Xie Q. Geochemical reactions-induced hydrogen loss during underground hydrogen storage in sandstone reservoirs. Int J Hydrogen Energy. 2021;46:19998-20009.

[15] Bensing JP, Misch D, Skerbisch L, Sachsenhofer RF. Hydrogen-induced calcite dissolution in Amaltheenton Formation claystones: Implications for underground hydrogen storage caprock integrity. Int J Hydrogen Energy. 2022;47:30621-6.

[16] Zhan S, Zeng L, Al-Yaseri A, Sarmadivaleh M, Xie Q. Geochemical modelling on the role of redox reactions during hydrogen underground storage in porous media. Int J Hydrogen Energy. 2023.

[17] Haddad P, Ranchou-Peyruse M, Guignard M, Mura J, Casteran F, Ronjon-Magand L, et al. Geological storage of hydrogen in deep aquifers–an experimental multidisciplinary study. Energy & Environmental Science. 2022;15:3400-15.

[18] Tremosa J, Jakobsen R, Le Gallo Y. Assessing and modeling hydrogen reactivity in underground hydrogen storage: A review and models simulating the Lobodice town gas storage. Frontiers in Energy Research. 2023;11:1145978.

[19] Hosseini M, Sedev R, Ali M, Ali M, Fahimpour J, Keshavarz A, et al. Hydrogen-wettability alteration of Indiana limestone in the presence of organic acids and nanofluid. Int J Hydrogen Energy. 2023.

[20] Zhao Q, Wang Y, Chen C. Numerical simulation of the impact of different cushion gases on underground hydrogen storage in aquifers based on an experimentally-benchmarked equation-of-state. Int J Hydrogen Energy. 2023.

[21] Gholami R. Hydrogen storage in geological porous media: Solubility, mineral trapping, H2S generation and salt precipitation. Journal of Energy Storage. 2023;59:106576.

[22] Yekta AE, Pichavant M, Audigane P. Evaluation of geochemical reactivity of hydrogen in sandstone: Application to geological storage. Appl Geochem. 2018;95:182-94.

[23] Hosseini M, Ali M, Fahimpour J, Keshavarz A, Iglauer S. Calcite–Fluid Interfacial Tension: H2 and CO2 Geological Storage in Carbonates. Energy & Fuels. 2023;37:5986-94.

[24] Hosseini M, Fahimpour J, Ali M, Keshavarz A, Iglauer S. H2− brine interfacial tension as a function of salinity, temperature, and pressure; implications for hydrogen geo-storage. Journal of Petroleum Science and Engineering. 2022;213:110441.

[25] Isfehani ZD, Sheidaie A, Hosseini M, Fahimpour J, Iglauer S, Keshavarz A. Interfacial tensions of (brine+ H2+ CO2) systems at gas geo-storage conditions. J Mol Liq. 2023;374:121279.

[26] Pereira LM, Chapoy A, Burgass R, Oliveira MB, Coutinho JA, Tohidi B. Study of the impact of high temperatures and pressures on the equilibrium densities and interfacial tension of the carbon dioxide/water system. The Journal of Chemical Thermodynamics. 2016;93:404-15.

[27] Chabab S, Théveneau P, Coquelet C, Corvisier J, Paricaud P. Measurements and predictive models of high-pressure H2 solubility in brine (H2O+NaCl) for underground hydrogen storage application. Int J Hydrogen Energy. 2020;45:32206-20.

[28] Torín-Ollarves GA, Trusler JM. Solubility of hydrogen in sodium chloride brine at high pressures. Fluid Phase Equilib. 2021;539:113025.

[29] Peper S, Fonseca JM, Dohrn R. High-pressure fluid-phase equilibria: Trends, recent developments, and systems investigated (2009–2012). Fluid Phase Equilib. 2019;484:126-224.

[30] Caumon M-C, Sterpenich J, Randi A, Pironon J. Measuring mutual solubility in the H2O–CO2 system up to 200 bar and 100 C by in situ Raman spectroscopy. Int J Greenhouse Gas Control. 2016;47:63-70.

[31] dos Santos PF, André L, Ducousso M, Contamine F, Cézac P. Experimental measurement of CO2 solubility in aqueous Na2SO4 solution at temperatures between 303.15 and 423.15 K and pressures up to 20 MPa. J Chem Eng Data. 2020;65:3230-9.

[32] Al Ghafri S, Maitland GC, Trusler JM. Densities of aqueous MgCl2 (aq), CaCl2 (aq), KI (aq), NaCl (aq), KCl (aq), AlCl3 (aq), and (0.964 NaCl+ 0.136 KCl)(aq) at temperatures between (283 and 472) K, pressures up to 68.5 MPa, and molalities up to 6 mol· kg–1. J Chem Eng Data. 2012;57:1288-304.

[33] Leachman JW, Jacobsen RT, Penoncello S, Lemmon EW. Fundamental equations of state for parahydrogen, normal hydrogen, and orthohydrogen. J Phys Chem Ref Data. 2009;38:721-48.

[34] Lemmon E, Bell IH, Huber M, McLinden M. NIST Standard Reference Database 23: Reference Fluid Thermodynamic and Transport Properties-REFPROP, Version 10.0. National Institute of Standards and Technology. 2018.

[35] Søreide I, Whitson CH. Peng-Robinson predictions for hydrocarbons, CO2, N2, and H2S with pure water and NaCl brine. Fluid Phase Equilib. 1992;77:217-40.

[36] Chabab S, Cruz JL, Poulain M, Ducousso M, Contamine F, Serin JP, et al. Thermodynamic Modeling of Mutual Solubilities in Gas-Laden Brines Systems Containing CO2, CH4, N2, O2, H2, H2O, NaCl, CaCl2, and KCl: Application to Degassing in Geothermal Processes. Energies. 2021;14:5239.

[37] Taylor BN, Kuyatt CE. NIST Technical Note 1297: guidelines for evaluating and expressing the uncertainty of NIST measurement results. National Institute for Standards and Technology. Gaithersburg, MD1994.

[38] Ahmadi P, Chapoy A. CO2 solubility in formation water under sequestration conditions. Fluid Phase Equilib. 2018;463:80-90.

[39] Shah MK, Fisher R, Hassan I, Makarov E, Medvedev O, Memon A. Measuring reservoir fluid composition using a novel continuous contact flash method based on a microfluidic device. Abu Dhabi International Petroleum Exhibition and Conference: SPE; 2015. p. D041S63R05.

[40] Parkhurst DL, Appelo C. Description of input and examples for PHREEQC version 3—a computer program for speciation, batch-reaction, one-dimensional transport, and inverse geochemical calculations. US geological survey techniques and methods. 2013;6:497.

[41] Sandler SI. Chemical, biochemical, and engineering thermodynamics: John Wiley & Sons; 2017.

[42] Michelsen ML, Mollerup J. Thermodynamic modelling: fundamentals and computational aspects: Tie-Line Publications; 2004.

[43] Poling BE, Prausnitz JM, O'connell JP. Properties of gases and liquids: McGraw-Hill Education; 2001.

[44] Firoozabadi A. Thermodynamics of hydrocarbon reservoirs: McGraw-Hill; 1999.

[45] Chen CC, Britt HI, Boston J, Evans L. Local composition model for excess Gibbs energy of electrolyte systems. Part I: Single solvent, single completely dissociated electrolyte systems. AIChE Journal. 1982;28:588-96.

[46] Chen CC, Evans LB. A local composition model for the excess Gibbs energy of aqueous electrolyte systems. AIChE journal. 1986;32:444-54.

[47] Austgen DM, Rochelle GT, Peng X, Chen CC. Model of vapor-liquid equilibria for aqueous acid gas-alkanolamine systems using the electrolyte-NRTL equation. Industrial & engineering chemistry research. 1989;28:1060-73.

[48] Posey ML. Thermodynamic model for acid gas loaded aqueous alkanolamine solutions: The University of Texas at Austin; 1996.

[49] Bishnoi S, Rochelle GT. Physical and chemical solubility of carbon dioxide in aqueous methyldiethanolamine. Fluid Phase Equilib. 2000;168:241-58.

[50] Dash SK, Samanta AN, Bandyopadhyay SS. Solubility of carbon dioxide in aqueous solution of 2-amino-2-methyl-1-propanol and piperazine. Fluid Phase Equilib. 2011;307:166-74.

[51] Hessen ET, Haug-Warberg T, Svendsen HF. The refined e-NRTL model applied to CO2–H2O–alkanolamine systems. Chem Eng Sci. 2010;65:3638-48.

[52] Plakia A, Voutsas E. Modeling of H2S, CO2+ H2S, and CH4+ CO2 solubilities in aqueous monoethanolamine and methyldiethanolamine solutions. Industrial & Engineering Chemistry Research. 2020;59:11317-28.

[53] Pitzer KS, Simonson JM. Thermodynamics of multicomponent, miscible, ionic systems: theory and equations. J Phys Chem. 1986;90:3005-9.

[54] Robinson RA, Stokes RH. Electrolyte solutions: Courier Corporation; 2002.

[55] Rashin AA, Honig B. Reevaluation of the Born model of ion hydration. J Phys Chem. 1985;89:5588-93.

[56] Peng D-Y, Robinson DB. A new two-constant equation of state. Ind Eng Chem Fundam. 1976;15:59-64.

[57] Song Y, Chen C-C. Symmetric electrolyte nonrandom two-liquid activity coefficient model. Industrial & Engineering Chemistry Research. 2009;48:7788-97.

[58] Baudouin O, Dechelotte S, Guittard P, Vacher A. Simulis® Thermodynamics: an open framework for users and developers. Computer Aided Chemical Engineering: Elsevier; 2008. p. 635-40.

[59] Simulis Thermodynamics - ProSim. https://www.prosim.net/en/product/simulis-thermodynamics-mixture-properties-and-fluid-phase-equilibria-calculations/

[60] Zhu Z, Cao Y, Zheng Z, Chen D. An Accurate Model for Estimating H2 Solubility in Pure Water and Aqueous NaCl Solutions. Energies. 2022;15:5021.

[61] Duan Z, Sun R, Zhu C, Chou I-M. An improved model for the calculation of CO2 solubility in aqueous solutions containing Na+, K+, Ca2+, Mg2+, Cl−, and SO42−. Mar Chem. 2006;98:131-9.

[62] Pitzer KS. Thermodynamics of electrolytes. I. Theoretical basis and general equations. J Phys Chem. 1973;77:268-77.

[63] Wagner W, Pruß A. The IAPWS formulation 1995 for the thermodynamic properties of ordinary water substance for general and scientific use. J Phys Chem Ref Data. 2002;31:387-535.

[64] Braun L. Über die Absorption von Stickstoff und von Wasserstoff in wässerigen Lösungen verschieden dissociierter Stoffe. Z Phys Chem. 1900;33:721-39.

[65] Crozier TE, Yamamoto S. Solubility of hydrogen in water, sea water, and sodium chloride solutions. J Chem Eng Data. 1974;19:242-4.

[66] Gillespie P, Wilson G. GPA Research Report RR-41 Gas Processors Association. Tulsa, OK. 1980.

[67] Afanasyev A, Vedeneeva E. Compositional modeling of multicomponent gas injection into saline aquifers with the MUFITS simulator. Journal of Natural Gas Science and Engineering. 2021:103988.

[68] Schlumberger P. PVTi and ECLIPSE 300: An Introduction to PVT analysis and Compositional Simulation. PVTi and Eclipse. 2005;300.

[69] Petitfrere M, Patacchini L, de Loubens R. Three-phase EoS-based Reservoir Simulation with Salinity Dependent Phase-equilibrium Calculations. ECMOR XV-15th European Conference on the Mathematics of Oil Recovery2016.

[70] Chabab S. Thermodynamic study of complex systems containing gas, water, and electrolytes: application to underground gas storage: Université Paris sciences et lettres; 2020.

[71] Ballentine CJ, Burgess R, Marty B. Tracing fluid origin, transport and interaction in the crust. 2002.

[72] Koschel D, Coxam J-Y, Rodier L, Majer V. Enthalpy and solubility data of CO 2 in water and NaCl (aq) at conditions of interest for geological sequestration. Fluid Phase Equilib. 2006;247:107-20.

[73] Krishnan C, Friedman HL. Model calculations for Setchenow coefficients. J Solution Chem. 1974;3:727-44.

[74] Prausnitz JM, Lichtenthaler RN, De Azevedo EG. Molecular thermodynamics of fluid-phase equilibria: Pearson Education; 1998.

[75] Huang P. Humidity standard of compressed hydrogen for fuel cell technology. ECS Transactions. 2008;12:479.

[76] Hancke R, Holm T, Ulleberg Ø. The case for high-pressure PEM water electrolysis. Energy Convers Manage. 2022;261:115642.

[77] Wiebe R, Gaddy V. The solubility of hydrogen in water at 0, 50, 75 and 100° from 25 to 1000 atmospheres. Journal of the American Chemical Society. 1934;56:76-9.

[78] O'Sullivan TD, Smith NO. Solubility and partial molar volume of nitrogen and methane in water and in aqueous sodium chloride from 50 to 125. deg. and 100 to 600 atm. J Phys Chem. 1970;74:1460-6.